Unfolding of Titin Domains Studied by Molecular Dynamics Simulations

Mu Gao[a], Hui Lu[b] and Klaus Schulten[a] †
[a] *Department of Physics and Beckman Institute*
University of Illinois at Urbana-Champaign, IL 61801
[b] *Department of Bioengineering*
University of Illinois at Chicago, IL 60607

Abstract. Titin, a $\sim$1 μm long protein found in striated muscle myofibrils, possesses unique elastic properties. The extensible behavior of titin has been demonstrated in atomic force microscopy and optical tweezer experiments to involve the reversible unfolding of individual immunoglobulin-like (Ig) domains. We have used steered molecular dynamics (SMD), a novel computer simulation method, to investigate the mechanical response of single titin Ig domains upon stress. Simulations of stretching Ig domains I1 and I27 have been performed in a solvent of explicit water molecules. The SMD approach provides a detailed structural and dynamic description of how Ig domains react to external forces. Validation of SMD results includes both quantitative and quantitative agreement with AFM recordings. Furthermore, combining SMD with single molecule experimental data leads to a comprehensive understanding of Ig domains' mechanical properties. A set of backbone hydrogen bonds that link the domains' terminal β-strands play a key role in the mechanical resistance to external forces. Slight differences in architecture permit a mechanical unfolding intermediate for I27, but not for I1. Refolding simulations of I27 demonstrate a locking mechanism.

Keywords: titin, steered molecular dynamics, atomic force microscopy, fibronectin, immunoglobulin

Abbreviations: SMD – Steered Molecular Dynamics; AFM – Atomic Force Microscopy

† Corresponding author. Email: kschulte@ks.uiuc.edu.

1. Introduction

The giant muscle protein titin, also known as connectin, is a roughly 1 μm long macromolecule which spans over half of the muscle sarcomere and plays important roles in muscle contraction and passive elasticity as reviewed in (Wang, 1996; Erickson, 1997; Maruyama, 1997; Linke, 2000; Tskhovrebova and Trinick, 2002; Granzier and Labeit, 2002). This string-like molecule is primarily composed of ∼300 tandem repeats of two types of domains, immunoglobulin-like (Ig) domains and fibronectin type III (FnIII) domains, as well as of a unique region called PEVK that is rich in proline, glutamate, valine and lysine residues (Labeit and Kolmerer, 1995). Anchored at the Z-disk and at the M-line, titin develops a passive force which keeps sarcomere components uniformly organized during muscle contraction and restores sarcomere length when the muscle is relaxed. The I band part of titin is believed to be responsible for titin extensibility and passive elasticity. It consists mainly of two tandem regions of Ig domains (proximal Ig region and distal Ig region), separated by the PEVK region. Each of the Ig domains possesses about 100 amino acids built in a β-sandwich architecture. The PEVK region, however, mostly contains coiled conformations which are easily elongated when the muscle is stretched (Linke et al., 1998; Trombitas et al., 1998; Ma et al., 2001; Li et al., 2001b). It has been proposed that individual Ig domains also unfold to provide the necessary extension for muscle (Soteriou et al., 1993; Erickson, 1994). Recent studies have found that massive Ig domain unfolding cannot happen, rather, upon rapid stretching only a few of them unfold (Minajeva et al., 2001).

Titin domains have been manipulated, using single molecule techniques, in atomic force microscopy (AFM) (Rief et al., 1997; Carrion-Vazquez et al., 1999; Marszalek et al., 1999; Li et al., 2002) and optical tweezer (Kellermayer et al., 1997; Tskhovrebova et al., 1997) experiments, and found to possess protection against strain-induced domain unfolding. We refer to proteins which are designed to respond to force application under physiological conditions as *mechanical proteins*. Other proteins, which may not encounter mechanical strain under physiological conditions, have been found to exhibit little resistance against strain-induced unfolding, as has been demonstrated through AFM experiments on spectrin (Rief et al., 1999) and barnase (Best et al., 2001).

The AFM force-extension profiles of multimers of Ig domains (from titin) and FnIII (from titin, and also from tenascin and fibronectin) display a regularly repeated sawtooth pattern (Rief et al., 1997; Rief et al., 1998; Oberhauser et al., 1998; Oberhauser et al., 2002). The spacing between any two force peaks matches the extended length of one Ig or FnIII domain from its folded state, proving that, when these multi-domain proteins are stretched, their domains unfold one by one. The high magnitude of the force peaks, dependent on the pulling speed and type of protein, implies that the Ig and FnIII domains are designed to withstand significant stretching forces. At a pulling speed of 1 μm/s, for example, AFM unfolding of titin Ig domains requires about 200 pN while unfolding of FnIII domains requires a force ranging from 75 – 200 pN (Rief et al., 1997; Oberhauser et al., 2002). One remarkable property of these mechanical proteins is that they unfold reversibly. Refolding rates of around 1 s^{-1} were reported in AFM forced-unfolding experiments of titin I27 and FN-III_{10} (Rief et al., 1997; Carrion-Vazquez et al., 1999; Oberhauser et al., 2002).

The experimental observations required an interpretation in terms of the architecture of the titin modules. Currently, only two experimental structures of titin I-band Ig domains are available, the 1st Ig domain (Mayans et al., 2001) from the proximal Ig region and the 27th Ig domain (Improta et al., 1996) (according to the new nomenclature (Freiburg et al., 2000), I27 is now termed I91) from the distal Ig region. These domains adopt the typical I-frame immunoglobulin super-family fold (Politou et al., 1995), consisting of two β-sheets packed against each other, as shown in Figure 1, with each sheet containing four or five β-strands. One sheet comprises strands A, B, E, and D, the other sheet comprises strands A', G, F, C, and C' (the latter in I1 only). All adjacent β-strands in both sheets are anti-parallel to each other, except for the parallel pair A' and G. The β-strands A and A' belong to different sheets but are part of the N-terminal strand. Both structures are stabilized by hydrophobic core interactions between the two β-sheets and by hydrogen bonds between β-strands. One major

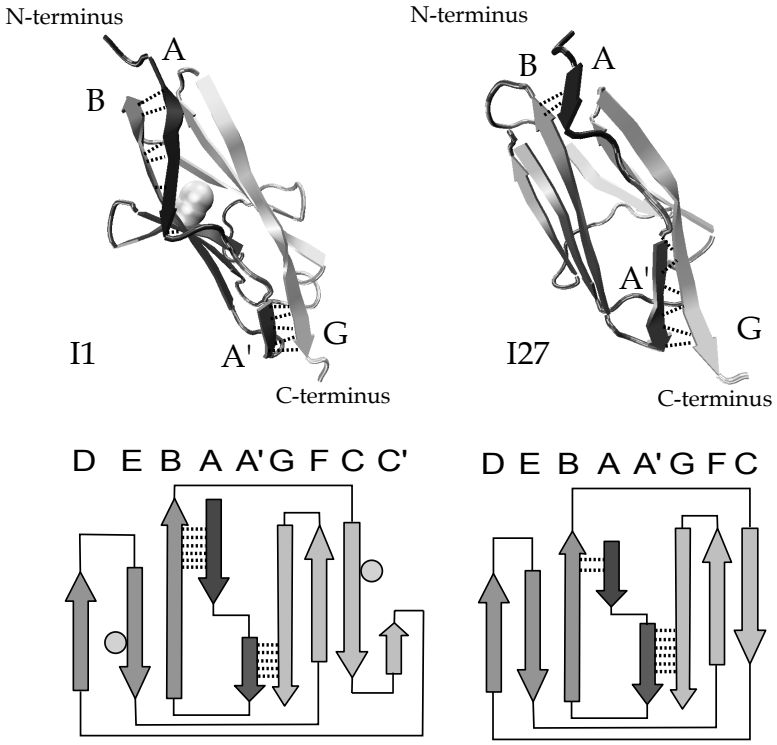

Figure 1. Structures and topology diagrams of I1 and I27 domains. β-strand A and A' are shown in black, other β-strands are shown in grey. Essential inter-strand hydrogen bonds for the mechanical stability of titin modules are represented as black dashed lines. The cysteine residues forming a disulfide bridge in I1 are represented as circles.

structural difference between I1 and I27, however, is that I1 contains a pair of cysteines which form a disulfide bridge under oxidizing conditions between two β-sheets, whereas I27 seems to lack the potential to form a disulfide bridge, even though I27 contains two cysteine residues.

While single molecule experiments provide valuable dynamic force spectroscopy for mechanical proteins, the corresponding conformational changes of stretched proteins cannot be observed directly because conventional structure resolving methods such as X-ray and NMR are not applicable. SMD is the method that is well positioned to address this problem and unveil the atomic-level pictures behind the saw-tooth like force profiles observed in AFM experiments. SMD, reviewed in (Isralewitz et al., 2001), is a novel approach to the study of the dynamics of biomolecular systems, especially for mechanical proteins. Starting from an equilibrated x-ray or NMR structure, the dynamics of the protein are recorded during force-induced unfolding simulations, thus providing a better understanding of the structure-function relationship of the simulated protein. The advantage of SMD over conventional molecular dynamics is the ability to induce relatively large conformational changes in molecules on the nanosecond time scales accessible to computation. Two main pulling protocols have been used in simulating Ig domain unfolding: constant velocity pulling and constant force pulling. Constant velocity pulling mimics the AFM experiment and, hence, allows one to compare SMD data with AFM recordings and to provide interpretation for experiments. Constant force pulling allows extensive studies of the barrier crossing event along the potential surface of the unfolding pathway. In combination with a statistical analysis, one can provide a quantitative description of the potential barrier separating the folded and unfolded domains and compare it to experimental observations.

In this paper we summarize the results of molecular dynamics simulations presented elsewhere (Lu et al., 1998; Lu and Schulten, 1999b; Lu and Schulten, 1999a; Lu and Schulten, 2000; Gao et al., 2001; Gao et al., 2002b) to provide an overall view of the reversible unfolding of titin modules.

2. Methods

The Ig domain structures, I27 and I1, obtained from the protein data bank entry 1TIT and 1G1C, were employed in this modeling study. To simulate a solvent environment, the Ig domain structures were surrounded by a sphere of water molecules, which covered the molecular surface of the domain by at least four shells of water molecules, resulting in systems of 12,000 to 18,000 atoms.

The MD simulations were performed using the programs X-PLOR (Brünger, 1992) and NAMD (Kalé et al., 1999) with the CHARMm22 force field (MacKerell Jr. et al., 1998), assuming an integration time step of 1 fs and a uniform dielectric constant of 1. The non-bonded van der Waals (vdW) and Coulomb interactions were calculated with a cut-off using a switching function starting at a distance of 10 Å and reaching zero at 13 Å. The TIP3P water model was employed for the solvent (Jorgensen et al., 1983).

Two SMD protocols, constant-velocity and constant force stretching, have been applied to titin modules. SMD using constant-velocity moving restraints simulates the stretching of protein domains with a moving AFM cantilever. One terminus is fixed during the simulation, which prevents the protein from simply translating in space when external forces are applied, and this corresponds to attaching the protein to a fixed substrate in the AFM experiments. The other terminus is restrained to a point in space (restraint point) by an external, e.g., harmonic, potential. The restraint point is then shifted in a chosen direction (Grubmüller et al., 1996; Isralewitz et al., 1997; Lu et al., 1998), forcing the restrained terminus to move from its initial position. Assuming a single reaction coordinate x and an external potential $U = k(x - x_0 - vt)^2/2$, where x_0 is the initial position of the restraint point moving with a constant velocity v, and k is the stiffness of the restraint, the external force exerted on the system can be expressed as

$$F = k(x_0 + vt - x)\,. \tag{1}$$

This force corresponds to a protein being pulled by a harmonic spring of stiffness k with one end attached to the restrained terminus and the other end moving with velocity v. The force applied in constant force SMD retains the same direction and magnitude regardless of the position of the restrained terminus.

SMD simulations with constant velocity stretching were carried out on I1 and I27 by fixing the C_α atoms of the N-terminal residue, and by applying external forces to the C_α atom of the C-terminal residue. The value of k was set to 7 $k_BT/Å^2$, corresponding to spatial (thermal) fluctuations of the constrained C_α atom with variance $\delta x = \sqrt{k_BT/k} = 0.38$ Å at $T = 300\ K$. SMD simulations with constant force stretching were implemented by fixing the N-terminus of the Ig domains and by applying a constant force to the C-terminus along the direction connecting the initial positions of the N-terminus to the C-terminus.

3. Results

The results of forced unfolding of I1 (oxidized and reduced) and I27 with constant velocity stretching are compared in Fig. 2a. I27 exhibits the major resistance to external forces in the extension from 12–15 Å, where a dominant force peak arises. At extensions larger than 20 Å the domain exhibits little resistance against stretching as is evident from the fact that only relatively weak forces are needed to increase extension. The force-extension profiles from previous work (Lu and Schulten, 1999a; Gao et al., 2002b) have also shown that the lower the pulling speed, the lower the forces needed to extend the domain. A decrease of the speed from 0.5 Å/ps to 0.01 Å/ps reduces the peak force from 2500 pN to 1500 pN for I27. Since the current accessible timescale to SMD simulations, nanosecond, is about six orders of magnitude shorter than a millisecond over which unfolding of Ig domains occurs in AFM experiments, the peak forces calculated in SMD simulations are larger than those measured in AFM experiments (Lu et al., 1998; Lu and Schulten, 1999a). Despite this the simulated force-extension

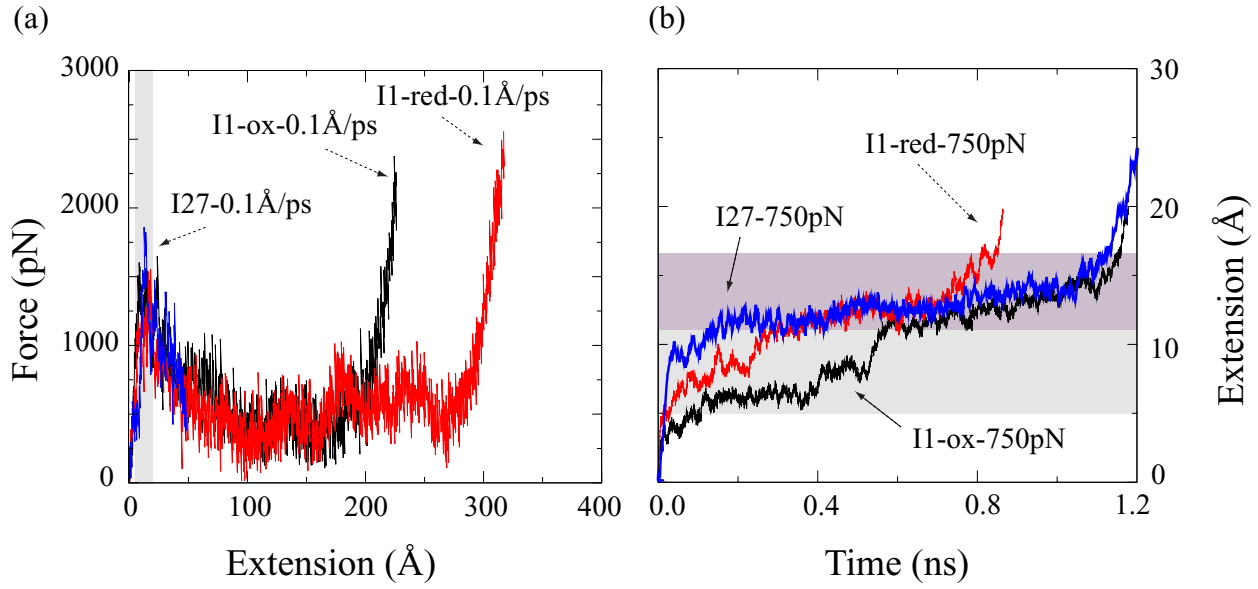

Figure 2. (a) Force-extension profiles from SMD simulations with 0.1 Å/ps constant velocity stretching of oxidized I1 (black), reduced I1 (red) and I27 (blue). The gray area highlights the region where the force peak arises. (b) Extension-time profiles from SMD simulations with 750 pN constant force stretching of oxidized I1, reduced I1 and 27. The shaded areas correspond to key transition states for crossing barriers formed by hydrogen bonds between A- and B-strands (light gray) and by hydrogen bonds between A' and G-strands (dark gray).

curves share the main qualitative feature with those observed in AFM stretching experiments: a single dominant force peak. I1 domains exhibit strong resistance against external forces in the extension range 5–16 Å, which is broader than the main burst region of I27. However, the unfolding force peak of I1 is lower than that of I27. For example, at 0.1 Å/ps pulling speed unfolding of I1 requires a peak force that is about 300 pN lower than that of unfolding I27. This implies that I1 is slightly less stable than I27. Similar to I27, unraveling I1 to extensions beyond the main force peak, which corresponds to the unfolding barrier, requires weaker and weaker forces until the protein backbone is completely extended when forces rise again. Since oxidized I1 contains a disulfide bond, the domain can only extend to ∼220 Å as shown in Fig. 2a, whereas reduced I1 can be stretched to ∼300 Å, the length of a fully extended I1 domain.

Although constant velocity simulations reproduced a qualitatively similar force-extension profile as seen in AFM experiments, revealing the key factor that determines the unfolding barrier and obtaining a quantitative comparison to experimental data is difficult to achieve from such approach because the proteins pass the transition state very quickly, typically in less than 100 ps. To address these issues, we have introduced constant force simulations in which forces much lower than the peak unfolding force calculated from constant velocity simulations were applied. During constant force simulations the proteins were hindered in front of the unfolding barrier for up to several ns, thus allowing us to capture the key events that characterize the barrier crossing (Lu and Schulten, 1999a). Moreover, with the mean first passage time theory we are capable to calculate the height of the unfolding barrier that can be compared with experimental results.

An analysis of the constant force simulation trajectories corresponding to the profiles shown in Fig. 2b reveals that I27 unfolds in two key steps (Marszalek et al., 1999; Lu and Schulten, 1999a). At the first step, an initial 12 Å extension takes place due to a straightening of the polypeptide chain near its terminal ends and disruption of the two hydrogen bonds between β-strands A and B. This extension, shown in Fig. 2b for 750pN stretching, continues until a plateau region (which is longer for weaker forces) is reached, at which point the six A'-G inter-strand hydrogen bonds come under mechanical strain. At the second step, the domain extensions fluctuate around a constant value

during the plateau period, until the A'-G bonds concurrently break, after which the extension rapidly increases. Similarly, unfolding I1 also involves rupture of both A-B and A'-G hydrogen bonds (Gao et al., 2002b). Compared to I27, however, disrupting the A-B bonds takes longer, for there are six A-B hydrogen bonds in I1. The main resistance of I1 is attributed to its six A-B bonds, especially for reduced I1 in which the disulfide bridge is absent. Under oxidizing conditions, the formation of the disulfide bond increases the stability of I1 by stabilizing A'-G bonds. After the A-B and A'-G bonds are broken, I1 and I27 unravel rapidly, with little resistance to the rupture of interstrand hydrogen bond that occurs in a zipper-like, i.e., one-by-one, fashion.

The plateaus shown in Fig. 2b correspond to barrier crossing processes, with $\tau_{barrier}$ denoting the mean first passage time spent at the plateau (Lu and Schulten, 1999a). The applied force effectively lowers the barrier such that stronger forces lead to faster barrier crossing than weaker forces. In all cases, the stretching motion gets temporarily "stuck" in front of the barrier, which can then only be overcome by thermal fluctuations. This scenario can be described as Brownian motion governed by a potential which is the sum of the indigenous barrier and a linear potential accounting for the applied force. The mean time to cross the barrier can be evaluated using the expressions for the mean first passage time developed in (Schulten et al., 1980; Szabo et al., 1980; Schulten et al., 1981). By comparing the mean first passage times with the respective times $\tau_{barrier}$ for various forces one can estimate the height of the indigenous potential barrier.

To estimate the shape of the indigenous potential barrier we assume a linearly increasing ramp model for the energy $U(x)$ of the barrier: $U(x) = \Delta U\,(x-a)/(b-a)$ for $a \le x \le b$. The dynamics of barrier crossing is described as a Brownian motion with a reflective boundary condition at a, and an absorptive boundary condition at b. Here ΔU is the height of the barrier, and $b-a$ the barrier width. This linear potential function should yield approximately the same $\tau_{barrier}$ as resulted from the indigenous barrier. The simple form of the model potential permits an analytical expression for the mean first passage time (Izrailev et al., 1997):

$$\tau(F) = 2\tau_d \delta(F)^{-2}[e^{\delta(F)} - \delta(F) - 1] \tag{2}$$

We have introduced here $\tau_d = (b-a)^2/2D$ and $\delta(F) = \beta[\Delta U - F(b-a)]$. Assuming a width of 3 Å, estimated from the fluctuation of the extension curves in Fig. 2, a least square fit procedure produces a value of 20.3 kcal/mol for the height of the unfolding barrier of I27 (Lu and Schulten, 1999a), in close agreement with AFM and denaturing experiments that suggest 22.2 kcal/mol (Carrion-Vazquez et al., 1999).

The constant force simulations also revealed an important mechanical difference between I1 and I27: I27 exhibits an intermediate of ∼7 Å extension (Marszalek et al., 1999), whereas I1 does not exhibit a similar intermediate (Gao et al., 2002b). Fig. 3 shows the extension of I1 and I27 in SMD simulations at constant forces of 50 pN and 200 pN applied for up to 10 ns. I1 appears less flexible than I27 as the force increased from 50 pN to 200 pN led to only ∼2 Å additional extension. Although two hydrogen bonds between β-strands A and B broke upon a constant force of 200 pN, further extension of I1 was restricted by the remaining four intact A-B hydrogen bonds (Fig. 3b). Obtaining additional extension for I1 requires breaking all six hydrogen bonds between A- and B-strands, which demands a larger force or longer stretching. In comparison, rupture of the two A-B hydrogen, bonds of I27 can result in ∼6 Å additional extension (Fig. 3c,d).

If Ig domains indeed unfold to fulfill their physiological roles, a rapid refolding rate is essential for their functions. Reversibly unfolding of Ig domains has been demonstrated in AFM experiments (Rief et al., 1997; Carrion-Vazquez et al., 1999). It takes about ∼1 sec for a fully stretched I27 domain to refold. The timescale, however, is too long to be reached in all-atom simulations. For practical purpose we simulate the refolding processes from structures that just crossed the main unfolding barrier (Gao et al., 2001). Fig. 4 presents reversible unfolding simulations of I27. The equilibrated protein was initially stretched with 750 pN constant force until all hydrogen bonds between A- and B-strands and between A'- and G-strands are broken (see snapshots on Fig. 4a). The force was then released, and

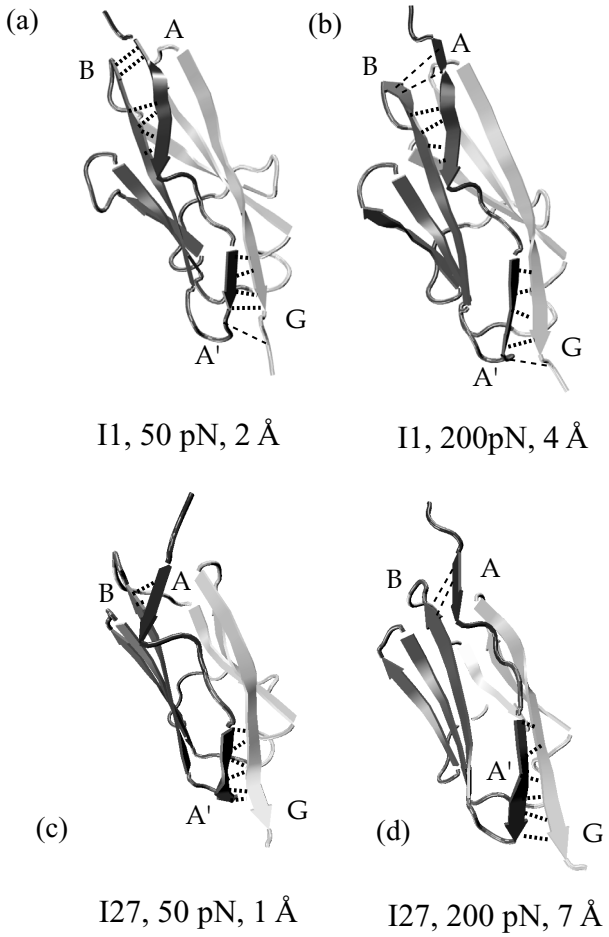

Figure 3. Snapshots of titin modules from SMD simulations with constant forces of 50 pN and 200 pN. Two hydrogen bonds between A- and B-strands of I27 are disrupted, while I1's six hydrogen bonds between A- and B-strands are intact.

the partially unfolded I27 was subsequently allowed to spontaneously relax. During the 2 ns refolding simulation, the domain became more compact with its extension decreasing from over 15 Å to 0 Å, the extension of the native fold. At the end of the refolding simulation, five of the six hydrogen bonds connecting A' and G reformed, except the bond between Y9(O) and N83(H) (see snapshots on Fig. 4b). One of two A-B hydrogen bonds was also reformed. Finally, a 750 pN force was applied to stretch the refolded protein, resulting in a barrier passage time of about 500 ps, similar to the passage time of unfolding native I27, indicating that a refolding close to the native structure has been achieved.

4. Discussion

Multi-domain proteins like titin constitute a fascinating class of biopolymers with important cellular functions. Single molecule AFM experiments that probe the mechanical response of these proteins provide a unique source of information that becomes more valuable in combination with steered molecular dynamics simulations. The latter provide atomic level pictures of the conformational changes governing the function of mechanical proteins which, however, need to be verified through comparison with experimental data.

Single molecule experiments (Rief et al., 1997; Kellermayer et al., 1997; Tskhovrebova et al., 1997; Marszalek et al., 1999; Li et al., 2002) have elucidated the chief design requirements for titin Ig domains

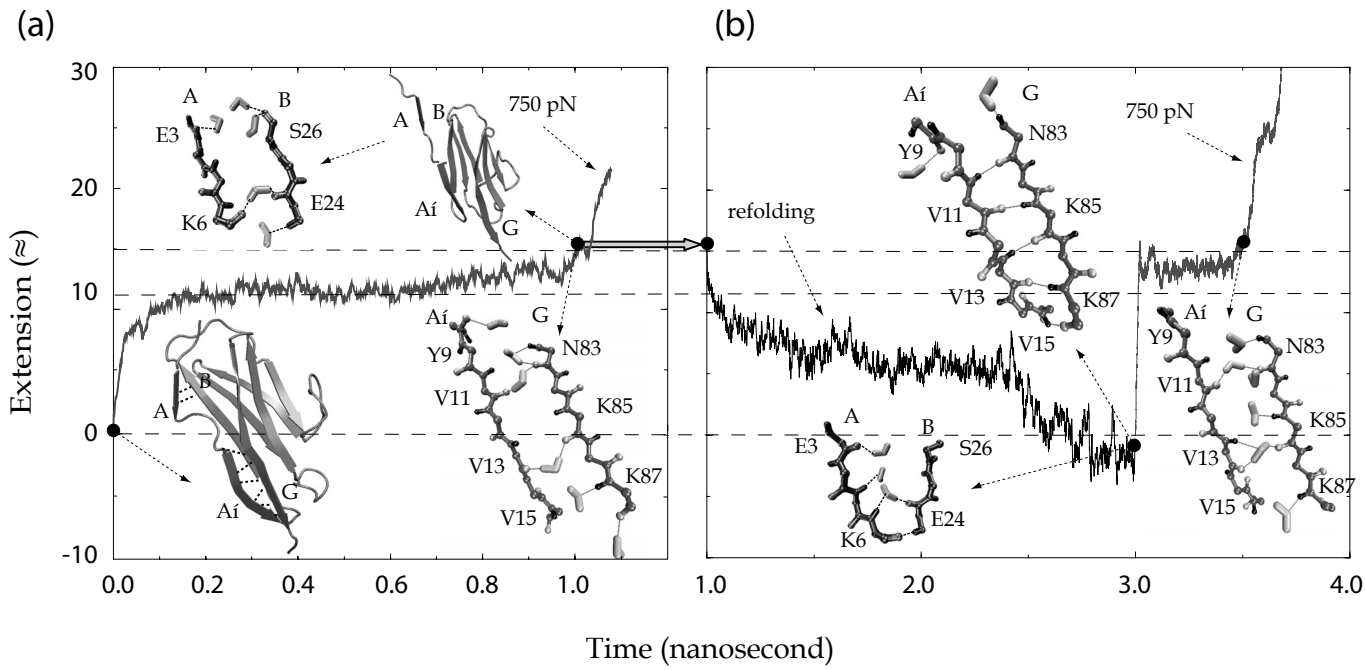

Figure 4. Extension profiles from a reversible unfolding simulation of I27, as well as snapshots of the protein and hydrogen bonding structure between A- and B-strands and between A'- and G-strands. (a) I27 was unfolded with 750 pN constant force. (b) At 1 ns, the force was released and the module was allowed to spontaneously refold for additional 2 ns. The force was then resumed to stretch the partially refolded protein.

under extreme stretch conditions: they unravel one by one, and increase the length of titin at each unraveling event by about 280 Å without affecting the stability of those domains which still remain folded. At small extensions of titin, when the link regions are pulled taut to form a straight chain, the Ig domains are at their resting contour length of about 40 Å. Upon SMD force application, distal Ig domains such as I27 and I28 exhibit a pre-burst increase in contour length of about 7 Å, while proximal Ig domains such as I1 do not show this pre-burst intermediate state (Li et al., 2002). With further extension, Ig domains continue to lengthen, but only after the force exceeds a given value. Our simulations provide an explanation for this bursting behavior. The links which must be ruptured to initiate the unfolding of the Ig domains are the backbone hydrogen bonds between β-strands A and B and between β-strands A' and G. Due to the topology of the Ig domain (Fig. 1), only when the A- and B-strands, as well as A'- and G-strands are separated, after breaking of all respective inter-strand hydrogen bonds, can the unfolding of an Ig domain continue, involving rupture of the inter-strand hydrogen bonds between the remaining β-strands. The AFM experiments have also found that unfolding distal Ig domains requires higher peak forces than unfolding proximal Ig domains (Li et al., 2002). This is probably because distal Ig domains have more concurrently breaking inter-strand hydrogen bonds than proximal Ig domains (see Fig. 1).

Ig domains, which exhibit high (>150 pN) dominant force peaks when stretched in AFM experiments and in SMD simulations, are called Class I proteins (Lu and Schulten, 1999b) (please note that this classification has nothing to do with the previous classification of the motifs of titin domains). Members belonging to this class exhibit strong resistance to forced unfolding; their fold topologies are such that interstrand hydrogen bonds must break in clusters in order to allow significant extension of the domain. Proteins like FN-III modules also belong to Class I. Simulations of FN-III modules revealed similar correlation between interstrand hydrogen bonds and mechanical stability of the modules (Krammer et al., 1999; Craig et al., 2001; Krammer et al., 2002; Gao et al., 2002a). Another example is ubiquitin, which exhibits multiple unfolding pathways (J. Fernandez, private communications). Other domains (e.g. all-helix domains or β proteins such as C2 domains) have

topologies that can be extended while breaking backbone hydrogen bonds individually. They do not exhibit dominant force peaks when stretched in SMD simulations(Lu and Schulten, 1999b); we call these class II domains. The study suggested that AFM experiments on class II proteins should exhibit force-extension profiles different from those performed on proteins consisting of several class I domains. Either no dominant force peak (and thus no fingerprints like the sawtooth pattern) or much lower force peak values than those observed for class I domains are expected. The discernible-but-lower force peak values observed in class II domains might arise from hydrophobic effects, which do not play an important role in force-induced unfolding of class I domains. Both possibilities, i.e., non-discernible (Carrion-Vazquez et al., 2000) and lower, discernible (Rief et al., 1999) peaks have already been observed in recent AFM experiments.

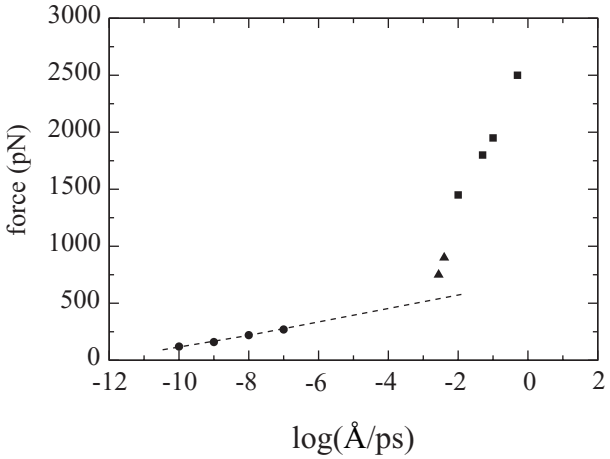

Figure 5. Force spectroscopy of unfolding I27 from AFM experiments (circle), constant velocity (square) and constant force SMD simulations (triangle). The velocities corresponding to constant force pulling were estimated as the length of the reaction region, about 3 Å, divided by the mean first passage time. Since the SMD simulations and AFM experiments belong to different regime, they have different scaling properties. However, decreasing the pulling velocity in SMD simulations yielded SMD data that tend towards the extrapolated AFM peak force curve.

The main obstacles to relating AFM measurements and MD simulations, namely the time scale discrepancy and the related discrepancy in unfolding forces, may be overcome through slower pulling speeds in the constant velocity SMD simulations. In this respect it is important to note that the slower 0.1 Å/ps and 0.01 Å/ps stretching simulations produce the same scenario of clustered hydrogen bond breaking as the faster 0.5 Å/ps simulation. On the other hand, the peak force values are reduced logarithmically. Fig. 5 shows that by reducing the pulling velocity the peak force data obtained from SMD simulations merge with the extrapolated AFM peak force curve. Even though it is not expected that the main unfolding scenario revealed by SMD simulations depends on pulling speed, further simulations with lower pulling speed are of great value, as we can then compare the force peak value quantitatively between SMD and AFM recordings.

Several different theoretical studies on forced unfolding of protein domains have also been published recently, employing approaches and methods different from ours. A molecular mechanics approach on α-helix and β-hairpin stretching study has been employed by Rohs *et al.* (Rohs et al., 1999). Stretching protein in reduced representation on a lattice model and an off-lattice model have been studied by Socci *et al.* (Socci et al., 1999) and by Klimov and Thirumalai (Klimov and Thirumalai, 1999; Klimov and Thirumalai, 2000). Evans and Ritchie (Evans and Ritchie, 1999) modeled the Ig domain unfolding as a single bond breaking event using the Kramers-Smoluchowski theory that also underlies our calculation of mean first passage times. Paci and Karplus (Paci and Karplus, 1999; Paci and Karplus, 2000) studied I27 and FnIII unfolding by means of biased molecular dynamics using an implicit solvent model to reduce computational effort; the authors suggested that the dominant barrier against unfolding is due

to vdW interactions, and not due to hydrogen bonds. Future SMD simulations will help clarify the differences among various theoretical approaches including those described above and will be aimed to provide a means to unite these approaches, while still relating them to experiments.

Our goal in modeling the stretching of titin domains is to obtain an atomic-level view of the process. Our resulting theoretical model should at least meet two criteria: first, the model should correspond closely to the experimental (AFM) situation, so as to provide a non-ambiguous check on the model's validity; second, the results should provide information on the process at atomic-level resolution that cannot be obtained from experiments. The SMD method has satisfied both criteria listed above. Force-extension curves produced by simulations can be directly compared to AFM data to examine the validity of the model. The SMD trajectories account for the unfolding process at atomic-level detail and, hence, reveal structure-dynamics-function relationships for protein elasticity properties not resolved by AFM.

SMD simulations can be used to help design proteins with unfolding barriers of desired strength. By mutating key residues involving forming A'-G hydrogen bonds of titin I27, for example, researchers have successfully created mutants that have fine tuned mechanical stabilities (Li et al., 2001a). Additionally, modeling force-sensitive proteins with SMD can provide insights into novel processes. For example, simulations of $FnIII_{10}$ revealed a mechanosensitive switch of the protein (Krammer et al., 1999; Krammer et al., 2002). Mechanical forces can make conformational changes of a loop containing the ligand Asp-Gly-Arg peptide so that the binding to integrin receptors is weakened. With more structures of mechanical proteins becoming available and simulated, SMD can contribute fundamentally to the understanding of structure-function relationships of mechanical proteins. Even for the giant protein titin, for example, by systematically simulating individual domains or segments and piecing together the results one can eventually understand how nature designs the elastic spring.

Acknowledgements

This work was supported by the National Institutes of Health Research grants PHS5P41RR05969 and 1R01GM60946, as well as the National Science Foundation supercomputer time grant NRAC MCA93S028.

References

Best, R. B., B. Li, A. Steward, V. Daggett, and J. Clarke: 2001, 'Can Non-Mechanical Proteins Withstand Force? Stretching Barnase by Atomic Force Microscopy and Molecular Dynamics Simulation'. *Biophys. J.* **81**, 2344–2356.

Brünger, A. T.: 1992, 'X-PLOR, Version 3.1: A System for X-ray Crystallography and NMR'. The Howard Hughes Medical Institute and Department of Molecular Biophysics and Biochemistry, Yale University.

Carrion-Vazquez, M., A. Oberhauser, S. Fowler, P. Marszalek, S. Broedel, J. Clarke, and J. Fernandez: 1999, 'Mechanical and chemical unfolding of a single protein: A comparison'. *Proc. Natl. Acad. Sci. USA* **96**, 3694–3699.

Carrion-Vazquez, M., A. F. Oberhauser, T. E. Fisher, P. E. Marszalek, H. Li, and J. M. Fernandez: 2000, 'Mechanical design of proteins studied by single-molecule force spectroscopy and protein engineering'. *Prog. Biophys. Mol. Biol.* **74**, 63–91.

Craig, D., A. Krammer, K. Schulten, and V. Vogel: 2001, 'Comparison of the early stages of forced unfolding of fibronectin type III modules'. *Proc. Natl. Acad. Sci. USA* **98**, 5590–5595.

Erickson, H.: 1994, 'Reversible unfolding of fibronectin type III and immunoglobulin domains provides the structural basis for stretch and elasticity of titin and fibronectin'. *Proc. Natl. Acad. Sci. USA* **91**, 10114–10118.

Erickson, H.: 1997, 'Stretching single protein modules: Titin is a weird spring'. *Science* **276**, 1090–1093.

Evans, E. and K. Ritchie: 1999, 'Strength of a Weak Bond Connecting Flexible Polymer Chains'. *Biophys. J.* **76**, 2439–2447.

Freiburg, A., K. Trombitas, W. Hell, O. Cazorla, F. Fougerousse, T. Centner, B. Kolmerer, C. Witt, J. Beckmann, C. Gregorio, H. Granzier, and S. Labeit: 2000, 'Series of exon-skipping events in the elastic spring region of titin as the structural basis for myofibrillar elastic diversity'. *Circ. Res.* **86**, 1114–1121.

Gao, M., D. Craig, V. Vogel, and K. Schulten: 2002a, 'Identifying Unfolding Intermediates of $FN\text{-}III_{10}$ by Steered Molecular Dynamics.'. *J. Mol. Biol.* Submitted.

Gao, M., H. Lu, and K. Schulten: 2001, 'Simulated Refolding of Stretched Titin Immunoglobulin Domains'. *Biophys. J.* **81**, 2268–2277.

Gao, M., M. Wilmanns, and K. Schulten: 2002b, 'Steered Molecular Dynamics Studies of Titin I1 Domain Unfolding.'. *Biophys. J.* In press.

Granzier, H. and S. Labeit: 2002, 'Cardiac titin: an adjustable multi-functional spring'. *J. Physiol.* **541**, 335–342.

Grubmüller, H., B. Heymann, and P. Tavan: 1996, 'Ligand Binding and Molecular Mechanics Calculation of the Streptavidin-Biotin Rupture Force'. *Science* **271**, 997–999.

Improta, S., A. Politou, and A. Pastore: 1996, 'Immunoglobulin-like modules from titin I-band: extensible components of muscle elasticity'. *Structure* **4**, 323–337.

Isralewitz, B., M. Gao, and K. Schulten: 2001, 'Steered Molecular Dynamics and Mechanical Functions of Proteins'. *Curr. Op. Struct. Biol.* **11**, 224–230.

Isralewitz, B., S. Izrailev, and K. Schulten: 1997, 'Binding Pathway of Retinal to Bacterio-opsin: A Prediction by Molecular Dynamics Simulations'. *Biophys. J.* **73**, 2972–2979.

Izrailev, S., S. Stepaniants, M. Balsera, Y. Oono, and K. Schulten: 1997, 'Molecular Dynamics Study of Unbinding of the Avidin-Biotin Complex'. *Biophys. J.* **72**, 1568–1581.

Jorgensen, W. L., J. Chandrasekhar, J. D. Madura, R. W. Impey, and M. L. Klein: 1983, 'Comparison of Simple Potential Functions for Simulating Liquid Water'. *J. Chem. Phys.* **79**, 926–935.

Kalé, L., R. Skeel, M. Bhandarkar, R. Brunner, A. Gursoy, N. Krawetz, J. Phillips, A. Shinozaki, K. Varadarajan, and K. Schulten: 1999, 'NAMD2: Greater Scalability for Parallel Molecular Dynamics'. *J. Comp. Phys.* **151**, 283–312.

Kellermayer, M., S. Smith, H. Granzier, and C. Bustamante: 1997, 'Folding-Unfolding Transition in Single Titin Modules Characterized With Laser Tweezers'. *Science* **276**, 1112–1116.

Klimov, D. K. and D. Thirumalai: 1999, 'Stretching single-domain proteins: Phase diagram and kinetics of force-induced unfolding'. *Proc. Natl. Acad. Sci. USA* **96**, 1306–1315.

Klimov, D. K. and D. Thirumalai: 2000, 'Native topology determines force-induced unfolding pathways in globular proteins'. *Proc. Natl. Acad. Sci. USA* **97**, 7254–7259.

Krammer, A., D. Craig, W. E. Thomas, K. Schulten, and V. Vogel: 2002, 'A structural model for force regulated integrin binding to fibronectin's RGD-synergy site'. *Matrix Biology* **21**, 139–147.

Krammer, A., H. Lu, B. Isralewitz, K. Schulten, and V. Vogel: 1999, 'Forced Unfolding of the Fibronectin Type III Module Reveals a Tensile Molecular Recognition Switch'. *Proc. Natl. Acad. Sci. USA* **96**, 1351–1356.

Labeit, S. and B. Kolmerer: 1995, 'Titins, giant proteins in charge of muscle ultrastructure and elasticity'. *Science* **270**, 293–296.

Li, H., W. Linke, A. F. Oberhauser, M. Carrion-Vazquez, J. G. Kerkvliet, H. Lu, P. E. Marszalek, and J. M. Fernandez: 2002, 'Reverse engineering of the giant muscle protein titin'. *Nature.* In Press.

Li, H., C. V. Mariano, A. F. Oberhauser, P. E. Marszalek, and J. M. Fernandez: 2001a, 'Point mutations alter the mechanical stability of immunoglobulin modules'. *Nature Struct. Biol.* **7**, 1117–1120.

Li, H., A. F. Oberhauser, S. D. Redick, M. Carrion-Vazquez, H. Erikson, and J. M. Fernandez: 2001b, 'Multiple conformations of PEVK proteins detected by single-molecule techniques'. *Proc. Natl. Acad. Sci. USA* **98**, 10682–10686.

Linke, W. A.: 2000, 'Stretching molecular springs: elasticity of titin filaments in vertebrate striated muscle'. *Histol. Histopathol.* **15**, 799–811.

Linke, W. A., M. Ivemeyer, P. Mundel, M. R. Stockmeier, and B. Kolmerer: 1998, 'Nature of PEVK-titin elasticity in skeletal muscle'. *Proc. Natl. Acad. Sci. USA* **95**, 8052–8057.

Lu, H., B. Isralewitz, A. Krammer, V. Vogel, and K. Schulten: 1998, 'Unfolding of Titin Immunoglobulin Domains by Steered Molecular Dynamics Simulation'. *Biophys. J.* **75**, 662–671.

Lu, H. and K. Schulten: 1999a, 'Steered Molecular Dynamics Simulation of Conformational Changes of Immunoglobulin Domain I27 Interpret Atomic Force Microscopy Observations'. *Chem. Phys.* **247**, 141–153.

Lu, H. and K. Schulten: 1999b, 'Steered Molecular Dynamics Simulations of Force-induced Protein Domain Unfolding'. *Proteins: Struct., Func., Gen.* **35**, 453–463.

Lu, H. and K. Schulten: 2000, 'The Key Event in Force-Induced Unfolding of Titin's Immunoglobulin Domains'. *Biophys. J.* **79**, 51–65.

Ma, K., L. Kan, and K. Wang: 2001, 'Polyproline II helix is a key structural motif of the elastic PEVK segment of titin'. *Biochemistry* **40**, 3427–38.

MacKerell Jr., A. D., D. Bashford, M. Bellott, R. L. Dunbrack Jr., J. Evanseck, M. J. Field, S. Fischer, J. Gao, H. Guo, S. Ha, D. Joseph, L. Kuchnir, K. Kuczera, F. T. K. Lau, C. Mattos, S. Michnick, T. Ngo, D. T. Nguyen, B. Prodhom, I. W. E. Reiher, B. Roux, M. Schlenkrich, J. Smith, R. Stote, J. Straub, M. Watanabe, J. Wiorkiewicz-Kuczera, D. Yin, and M. Karplus: 1998, 'All-hydrogen empirical potential for molecular modeling and dynamics studies of proteins using the CHARMM22 force field.'. *J. Phys. Chem. B* **102**, 3586–3616.

Marszalek, P. E., H. Lu, H. Li, M. Carrion-Vazquez, A. F. Oberhauser, K. Schulten, and J. M. Fernandez: 1999, 'Mechanical unfolding intermediates in titin modules'. *Nature* **402**, 100–103.

Maruyama, K.: 1997, 'Connectin/titin, a giant elastic protein of muscle'. *FASEB J.* **11**, 341–345.

Mayans, O., J. Wuerges, S. Canela, M. Gautel, and M. Wilmanns: 2001, 'Structural evidence for a possible role of reversible disulphide bridge formation in the elasticity of the muscle protein titin'. *Structure* **9**, 331–340.

Minajeva, A., M. Kulke, J. M. Fernandez, and W. A. Linke: 2001, 'Unfolding of Titin Domains Explains the Viscoelastic Behavior of Skeletal Myofibrils'. *Biophys. J.* **80**, 1442–1451.

Oberhauser, A., C. Badilla-Fernandez, M. Carrion-Vazquez, and J. Fernandez: 2002, 'The mechanical hierarchies of fibronectin observed with single molecule AFM'. *J. Mol. Biol.* **319**, 433–447.

Oberhauser, A. F., P. E. Marszalek, H. Erickson, and J. Fernandez: 1998, 'The molecular elasticity of tenascin, an extracellular matrix protein'. *Nature* **393**, 181–185.

Paci, E. and M. Karplus: 1999, 'Forced Unfolding of Fibronectin Type 3 Modules: An Analysis by Biased Molecular Dynamics Simulations'. *J. Mol. Biol.* **288**, 441–459.

Paci, E. and M. Karplus: 2000, 'Unfolding proteins by external forces and temperature: The importance of topology and energetics'. *Proc. Natl. Acad. Sci. USA* **97**, 6521–6526.

Politou, A. S., D. Thomas, and A. Pastore: 1995, 'The folding and the stability of titin immunoglobulin-like modules, with implications for mechanism of elasticity'. *Biophys. J.* **69**, 2601–2610.

Rief, M., M. Gautel, F. Oesterhelt, J. M. Fernandez, and H. E. Gaub: 1997, 'Reversible unfolding of individual titin immunoglobulin domains by AFM'. *Science* **276**, 1109–1112.

Rief, M., M. Gautel, A. Schemmel, and H. Gaub: 1998, 'The mechanical Stability of Immunoglobulin and Fibronectin III Domains in the Muscle Protein Titin Measured by AFM'. *Biophys. J.* **75**, 3008–3014.

Rief, M., J. Pascual, M. Saraste, and H. Gaub: 1999, 'Single molecule force spectroscopy of spectrin repeats: Low unfolding forces in helix bundles'. *J. Mol. Biol.* **286**, 553–561.

Rohs, R., C. Etchebest, and R. Lavery: 1999, 'Unraveling Proteins: A Molecular Mechanics Study'. *Biophys. J.* **76**, 2760–2768.

Schulten, K., Z. Schulten, and A. Szabo: 1980, 'Reactions Governed by a Binomial Redistribution Process. The Ehrenfest Urn Problem'. *Physica* **100A**, 599–614.

Schulten, K., Z. Schulten, and A. Szabo: 1981, 'Dynamics of Reactions Involving Diffusive Barrier Crossing'. *J. Chem. Phys.* **74**, 4426–4432.

Socci, N., J. Onuchic, and P. Wolynes: 1999, 'Stretching lattice models of protein folding'. *Proc. Natl. Acad. Sci. USA* **96**, 2031–2035.

Soteriou, A., A. Clarke, S. Martin, and J. Trinick: 1993, 'Titin folding energy and elasticity'. *Proc. R. Soc. Lond. B. (Biol. Sci.)* **254**, 83–86.

Szabo, A., K. Schulten, and Z. Schulten: 1980, 'First Passage Time Approach to Diffusion Controlled Reactions'. *J. Chem. Phys.* **72**, 4350–4357.

Trombitas, K., M. Greaser, S. Labeit, J. Jin, M. Kellermayer, M. Helmes, and H. Granzier: 1998, 'Titin Extensibility In Situ: Entropic Elasticity of Permanently Folded and Permanently Unfolded Molecular Segments'. *J. Cell Biol.* **140**, 853–859.

Tskhovrebova, L. and J. Trinick: 2002, 'Role of titin in vertebrate striated muscle'. *Proc. R. Soc. Lond. B. (Biol. Sci.)* **357**, 199–206.

Tskhovrebova, L., J. Trinick, J. Sleep, and R. Simmons: 1997, 'Elasticity and unfolding of single molecules of the giant protein titin'. *Nature* **387**, 308–312.

Wang, K.: 1996, 'Titin/connectin and Nebulin: Giant Protein Ruler of Muscle Structure And Function'. *Adv. Biophys.* **33**, 123–134.